Deanship of Graduate Studies
Al-Quds University

Formulation of a microemulsion of curcumin

Raghad Ziad Rasheed Zaghal

M.sc. Thesis

Jerusalem- Palestine

1447 /2025

Formulation of a microemulsion of curcumin

Prepared by:
Raghad Ziad Rasheed Zaghal

B.Sc. Nutrition and Food Processing/Hebron University. Palestine

Supervisor: Prof. Khawla Qamhieh
Co-Supervisor: Prof. Ibrahim Kayyali

A Thesis Submitted in partial fulfilment of requirements for the degree of Master of Chemical Industry in Applied and Industrial Technology Program/ Al-Quds University

1447 /2025

Al-Quds University

Deanship of Graduate Studies

Applied and Industrial Technology program

Thesis approval

Formulation of a microemulsion of curcumin

Prepared by: Raghad Ziad Rasheed Zaghal
Registration Number: 22112678

Supervisor: Prof. Khawla Qamhieh.
Co-Supervisor: Prof. Ibrahim Kayyali

Master thesis Submitted and Accepted, Date: 20.8.2025

The name and signature of examining committee member are as follows:

1- Prof. khawla qamhieh	Head of Committee,	Signature:
2- Prof. Ibrahim Kayyali	Co-Supervisor,	Signature:
3- Dr.Fouad Al Rimawi	Internal Examiner,	Signature: fuad rimawi
4- Dr.Ishaq Mousa	External Examiner,	Signature:

Jerusalem – Palestine.

1447 /2025

Dedication

I dedicate this thesis with profound love and gratitude to my parents, whose sacrifices, guidance, and prayers have shaped my path. To my siblings, for their endless encouragement and belief in me. And to my friends and mentors, who have supported me with patience and inspiration throughout this journey.

Raghad Zaghal

Declaration

I declare that my thesis is founded on independent research. Other researchers' work and findings are recorded and referenced. This thesis has never before been presented, in whole or in part, for any kind of academic degree. Prof. Khawla Qamhieh and oversaw the study, which was carried out at Al-Quds University in Jerusalem, Palestine.

Name: Raghad Ziad Rasheed Zaghal

Signed: 

Date:20.8.2025

Acknowledgment

Above all, I am grateful to Allah for providing me with the fortitude, endurance, and patience necessary to finish my thesis.

For looking for my baby and providing me with the time and peace of mind to concentrate on my education, I would especially want to thank my beloved mother and my husband's family. I am very grateful for your support and affection.

I want to truly thank my professors for their unwavering encouragement, support, and direction during my educational path. Their commitment and experience have been invaluable in helping to shape our effort.

I want to express my sincere gratitude to my friends Raghad and Riham for their kind help and support during the thesis process. Your compassion, support, and feedback meant a lot to me and helped me ease this trip.

Finally, I would want to express my gratitude to everyone who helped and encouraged me during this journey. All of you share in this achievement.

Raghad Zaghal

Abstract

Although curcumin is a bioactive compound with a wide range of pharmacological potential, its topical and systemic applications are severely limited by its poor water solubility. To enhance solubility and facilitate dermal delivery, a curcumin-loaded microemulsion system was developed using a nonionic surfactant blend of Span 80 and Tween 20, with ethanol as the co-surfactant and oleic acid as the oil phase. Curcumin was incorporated at a concentration of 3% (w/w). Pseudo-ternary phase diagram was constructed to identify single-phase microemulsion regions capable of effectively solubilizing curcumin. Several distinct zones of solubilization were observed, confirming the potential of this formulation approach for improving curcumin's solubility in both aqueous and oil phases.

Following the approach of Vollmer (1999), a fish-cut diagram was constructed to illustrate the relationship between temperature, composition, and curcumin solubility. To evaluate temperature effects on phase behavior, 16 samples were prepared using a binary mixture of 8 g oleic acid and 2 g distilled water. Each was combined with varying amounts (1.0–10.0 g and 6.3–7.8 g) of a ternary surfactant–curcumin solution prepared by dissolving 3 g of curcumin in 100 mL of 95% ethanol, followed by the addition of 50 mL Tween80 ,and 50 mL Span 80. Samples were subjected to different temperatures, and phase transitions were recorded. The resulting fish-cut diagram revealed a distinct solubilization region across various curcumin concentrations and temperature levels, marked as the "fish tail" region.

Experimental data were further used to calculate the water (R_w) and oil (R_o) droplet radii in both one-phase and two-phase regions. For R_w determination, the temperature was fixed at 45 °C, and measurements were taken at the specific water volume fraction corresponding to the intersection with the fish tail (Φ_w^{web}.), along with two preceding points in the two-phase region and one following point in the one-phase region. An increase in R_w was observed with increasing water content. A similar approach was used to determine R_o at a fixed temperature of 39 °C. The upper (T_u) and lower (T_l) phase transition temperatures were also determined, along with the corresponding Winsor boundary temperatures (T^{web} and T^{oeb}) for water and oil, respectively. The parameters a_w and a_o were calculated to determine the dimensionless micellar radii, $\frac{\left|R_{mic}^{oil}\right|}{l_s}$, $\frac{R_{mic}^{w}}{l_s}$, within the three-phase region. A plot was constructed to examine the relationship between the volume fraction of mixture A (Φ_A) and the normalized micellar radii, revealing a decreasing trend with increasing Φ_A. Additionally, the fish tail region was analyzed to explore correlations between T^{web} , T^{oeb}, and Φ_A. The water emulsification boundary (T^{web}) showed a linear increase with increasing volume fraction of A, while the oil emulsification boundary (T^{oeb}) exhibited a decreasing trend.

Overall, the findings demonstrate that the developed microemulsion significantly enhanced curcumin solubility and exhibited structural behavior consistent with established microemulsion theories. The integration of theoretical modeling with fish-cut diagram analysis proved to be a valuable approach for understanding and optimizing microemulsion systems. These results have practical implications for the development of pharmaceutical and cosmetic formulations of curcumin.

Keywords: Formulation, microemulsion, curcumin.

List of Contents

List of Tables:

List of Figures:

List of Abbreviations, Symbols and Terminology:

Abbreviation	Full word
WHO	World Health Organization
FDA	Food and Drug Administration
SMEs	submicron emulsions
nm	nanometer
o/w	oil-in-water
w/o	water-in-oil
CPP	critical packing parameter
v	lipophilic chain volume
a_0	cross-section area of hydrophilic head group
l_c	length of lipophilic chain
µg	microgram
cm	centimeter
mg	milligram
mL	milliliter
Curc-ME	curcumin microemulsion
pH	potential of hydrogen
ME	microemulsion
EE	entrapment efficiency
UHPLC	Ultra-High Performance Liquid Chromatography
SGIF	simulated gastrointestinal fluids
µS	microsiemens
PDI	polydispersity index
NMR	nuclear magnetic resonance spectroscopy
Wt.%	Weight percent
DI water	deionized water

ϕ	Phase
a_w	the change of the optimal radius of water with temperature
a_o	the change of the optimal radius of oil with temperature
$x\Phi_s$	the volume fraction of the hydrophilic head group of the surfactant molecule
R^{oil}_{mic}	the radii of oil micelles
R^{w}_{mic}	the radii of water micelles
T_l	Low temperature, the lowest temperature at which a microemulsion expels water.
T_u	Up temperature , the highest temperature where the 3ϕ region appears.
$x\, l_s$	the volume fraction of the hydrophilic head group of a surfactant molecule
l_s	Effective thickness of surfactant monolayer
A	Surfactant+co.Surfactant+Curcumin
Φ_A	Volume fraction of (Surfactant+co.Surfactant+Curcumin)
Φ_o	Volume fraction of oil
Φ_w	Volume fraction of water
T^{web}	Temperature related to water emulsification boundary
T^{oeb}	Temperature related to oil emulsification boundary
ln	Natural logarithm
oeb	oil emulsification boundary
web	water emulsification boundary
UV	ultraviolet
Vis	visible
Fig.	Figure
g	gram
°C	degrees Celsius
R_o	Oil droplet radius
R_w	Water droplet radius

R_{opt}^{w}	Optimal radius of water droplet
R_{opt}^{o}	Optimal radius of oil droplet
No.	number
Eq.	equation
v	volume
m	mass
ρ	density
Tv	Total volume
VA	volume of (Surfactant+Co.Surfactant+Curcumin)
Vw	volume of water
Vo	Volume of oil
O	oil
W	water
M.W	molecular weight
M	moles

Chapter One:

Introduction:

1.1 Curcumin

Curcumin is the principal bioactive compound found in turmeric (*Curcuma longa*), particularly concentrated in the rhizomes and tubers of plants such as Curcuma zedoaria and Acorus calamus. When extracted, curcumin appears as an orange-yellow crystalline powder with strong pigmentation properties. Chemically, it is classified as a diketone and polyphenolic compound, characterized by multiple conjugated double bonds, phenolic hydroxyl groups, and carbonyl groups—features that contribute to its wide range of biological activities.

Although curcumin is predominantly hydrophobic due to its non-polar aromatic rings and aliphatic chains, it is not entirely hydrophobic. The molecule contains three phenolic hydroxyl groups and two carbonyl groups, which enable limited hydrophilic interactions. At higher pH values, above its reported pKa values (~8.38, 9.88, and 10.51), the hydroxyl groups become deprotonated, thereby enhancing aqueous solubility and conferring partial hydrophilic behavior. Under acidic or neutral conditions, however, curcumin remains poorly soluble in water.

Commonly known as the "golden spice," turmeric has been used for thousands of years in South and Southeast Asia as both a culinary ingredient and a natural coloring agent. Beyond its culinary uses, turmeric has a long history of application in traditional medicine. Curcumin, the principal bioactive compound in turmeric, is recognized as a safe natural food additive by both the World Health Organization (WHO) https://apps.who.int/food-additives-contaminants-jecfa-database/Home/Chemical/638

and the U.S. Food and Drug Administration (FDA) https://www.hfpappexternal.fda.gov/scripts/fdcc/index.cfm?id=Curcumin&set=ColorAdditives

The "curcuminoid" family consists of three major polyphenolic compounds: curcumin (diferuloylmethane), demethoxycurcumin, and bisdemethoxycurcumin. Among these, curcumin is the most biologically active and has been the primary focus in the development of pharmaceuticals, dietary supplements, and functional food products.

Curcumin exhibits a broad spectrum of pharmacological properties, including anti-inflammatory, antioxidant, antitumor, antimicrobial, and wound-healing effects. Its therapeutic potential extends to cardiovascular and digestive health, largely attributed to its molecular structure and reactive functional groups. Several studies have demonstrated that curcumin exerts its anti-inflammatory and antioxidant effects by reducing pro-inflammatory markers.

Importantly, curcumin demonstrates selective cytotoxicity, showing greater cellular uptake and cytotoxic effects in cancerous cells compared to normal cells. This is believed to result from differences in protein expression and membrane composition between healthy and malignant cells. Curcumin also inhibits cell invasion, proliferation, angiogenesis, and metastasis while promoting cell cycle arrest and apoptosis in cancer cells.

Curcumin also inhibits cell invasion, proliferation, angiogenesis, and metastasis while promoting cell cycle arrest and apoptosis in cancer cells. Through the modulation of various signaling pathways and molecular targets, curcumin interferes with all three stages of carcinogenesis: initiation, promotion, and progression.

Despite its broad therapeutic potential, curcumin's clinical application has been limited by its low bioavailability when administered orally. This has led to the development of various formulation strategies—including nanoencapsulation and the use of bioenhancers such as piperine—to enhance its absorption and efficacy.

Given its safety profile—even at high doses up to 8 grams per day—and its wide range of biological activities, curcumin remains a highly promising candidate for further development as a therapeutic agent in modern medicine.

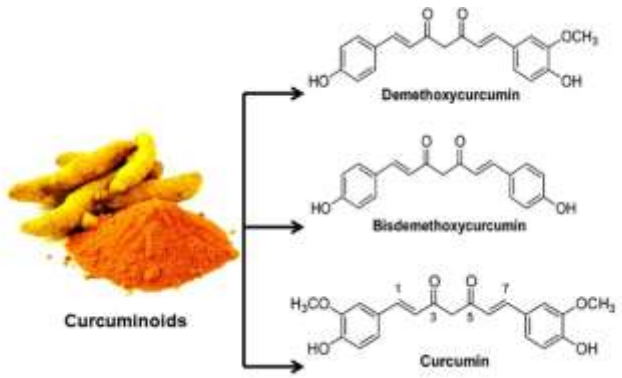

Fig.1.1: Molecular structure of curcumin.(Shalini Patle,M et al.2023)

1.2 Microemulsion

Microemulsions have garnered significant attention in recent decades due to their unique physicochemical properties and wide range of potential applications, particularly in pharmaceuticals, cosmetics, and chemical engineering. The concept of microemulsions was first introduced in the 1940s by Hoar and Schulman, who observed that titrating a milky emulsion with hexanol resulted in a clear, single-phase system. This early observation marked the beginning of extensive research into these thermodynamically stable and optically transparent or translucent systems.

A microemulsion is defined as a thermodynamically stable, isotropic liquid mixture composed of oil, water, surfactant, and typically a co-surfactant. The resulting dispersion is characterized by nanometer-sized droplets, generally ranging from 10 to 100 nm in diameter. Unlike conventional emulsions—which are thermodynamically unstable and tend to separate into distinct phases over time—microemulsions form spontaneously and remain stable under equilibrium conditions. This fundamental difference is crucial not only from a scientific standpoint but also in terms of practical applications, as microemulsions require significantly less energy to prepare, making them more economically viable for industrial-scale production.

The physical appearance of microemulsions also differs markedly from that of emulsions. While emulsions tend to appear cloudy or opaque due to their larger droplet size and light-scattering properties, microemulsions are typically transparent or translucent, a characteristic that can be advantageous in various applications, including drug delivery and diagnostics.

At the molecular level, conventional surfactants—comprising a hydrophilic (polar) head and a hydrophobic (apolar) tail—play a critical role in the formation and stabilization of microemulsions. In aqueous environments, surfactants self-assemble into a variety of equilibrium structures based on intermolecular interactions and entropic considerations. Interestingly, in non-aqueous or apolar solvents, such as alkanes, surfactants can also self-associate, albeit with an inverted molecular orientation. This reorientation minimizes the system's free energy and meets the solvation requirements of the surfactant molecules.

When surfactants are added to immiscible mixtures of oil and water, they localize at the interface, reducing interfacial tension and promoting the formation of stable microstructures. These systems can exhibit a range of phases, both macroscopic and microscopic. Microemulsions represent one such microscopic phase that is optically isotropic and thermodynamically stable. A variety of surfactant self-assembly structures that may arise in the presence of oil, water, or both are illustrated in Figure 1.2. While many of these structures hold promise for advanced applications such as drug delivery, such considerations fall outside the scope of the present study.

This thesis aims to explore the formation, characterization, and potential applications of microemulsions, with a focus on their thermodynamic properties, structural behavior, and relevance in pharmaceutical formulation.

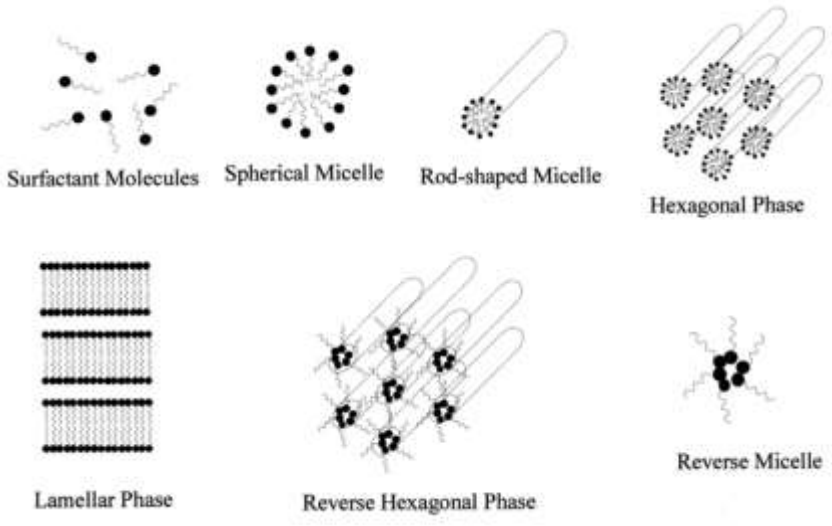

Fig.1.2 Schematic representation of the most commonly encountered self-association structures in water, oil or a combination thereof.(Lawrence, M. J, et al.2000)

1.3 Nanoemulsion

Nanoemulsions are a class of emulsified systems characterized by droplet sizes typically ranging between 50 and 1000 nanometers, with the most common average droplet size falling between 100 and 500 nm. Due to this size range, terms such as miniemulsions, submicron emulsions (SMEs), and ultrafine emulsions are often used interchangeably in the literature.

Since their development in the 1940s, nanoemulsions have been formulated in three primary types: **oil-in-water (o/w)**, **water-in-oil (w/o)**, and **bicontinuous** systems. Transformation between these types can be achieved by varying the emulsion composition or external conditions, such as temperature. Each form of nanoemulsion serves as a potential template for the synthesis of advanced polymeric materials, including **nonporous polymeric solids**, **latex particles**, and **functional polymer matrices**.

In pharmaceutical sciences, nanoemulsions have attracted growing interest as efficient delivery systems, particularly for **oral drug administration**. These formulations typically involve pharmaceutically approved components and offer a versatile platform for solubilizing poorly water-soluble drugs.

Nanoemulsions offer several notable advantages that make them highly attractive in pharmaceutical and biomedical applications. Their nanosized droplets provide enhanced drug delivery efficiency due to increased surface area and higher free energy, along with physical stability that minimizes the risks of creaming, flocculation, coalescence, or sedimentation. They are versatile in formulation, allowing the development of foams, creams, liquids, and sprays, and their non-toxic and non-irritant properties make them suitable for application on the skin and mucous membranes. In addition, they are feasible for oral administration when biocompatible surfactants are employed and are generally biocompatible, enabling use in both human and veterinary medicine without damaging healthy cells. Nanoemulsions also improve the absorption of oil-soluble compounds in cell culture technologies, facilitate toxicity studies on oil-based formulations, and can form

lamellar liquid crystalline phases around droplets, offering an alternative to liposomes and vesicles. Furthermore, their nanosized droplets enhance transdermal delivery by penetrating rough or irregular skin surfaces, and they serve as useful precursors for nanospheres and nanocapsules through techniques such as interfacial polycondensation and nanoprecipitation. Despite these benefits, nanoemulsions present certain limitations, including the need for high concentrations of surfactants and co-surfactants to achieve stability, sensitivity to pH and temperature which can compromise long-term storage, and the challenge of Ostwald ripening, a phenomenon where larger droplets grow at the expense of smaller ones, eventually leading to instability.

Phase Behavior and Droplet Size Control

Experimental studies on phase behavior have shown that the structure of the surfactant phase—whether a bicontinuous microemulsion or a lamellar phase—at the inversion point plays a critical role in controlling droplet size. This inversion point may be induced by changes in composition or temperature and is essential for designing stable nanoemulsion systems with targeted droplet characteristics.

Liposomes:

Liposomes are the phospholipid bilayer-enclosed spheres that form via self-assembly in water under the driving force of hydrophobicity.

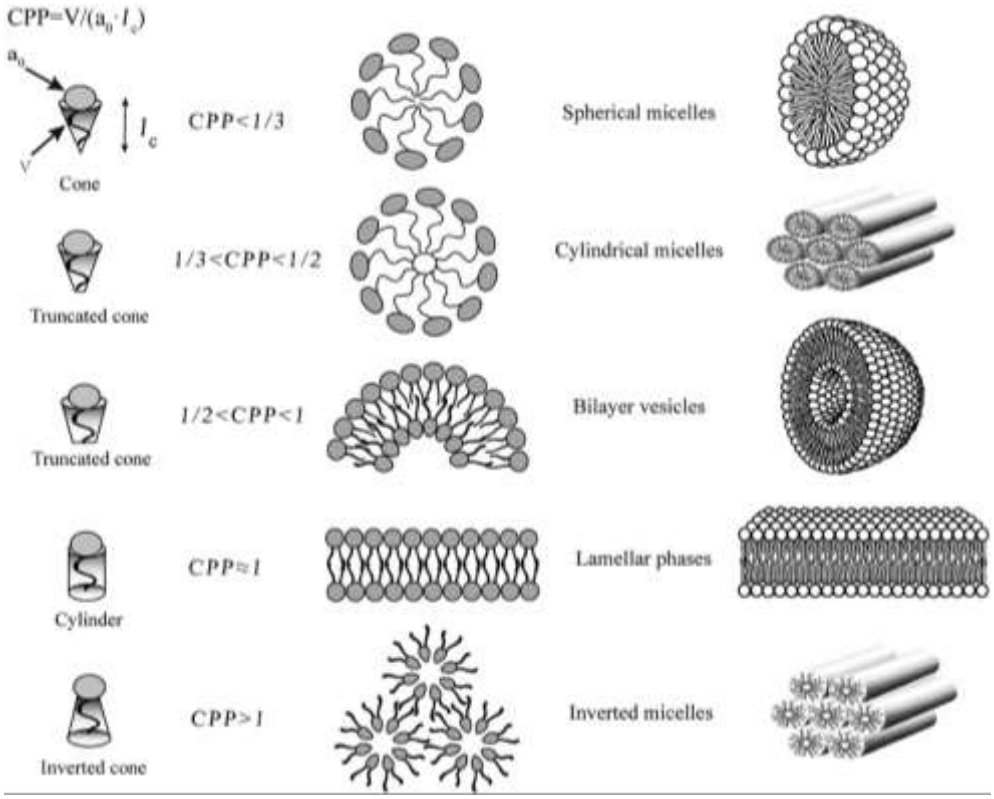

Fig.1.3 Molecular shape and critical packing parameter (CPP) of amphiphilic molecules, and the self-assembly entities formed of different amphiphiles.(Wang, N., et al.2019).

Liposomes have such a unique architecture that is constrained by the molecular shape of amphiphilic phospholipids, which have a critical packing parameter (CPP) in the range of from 1/2 to 1

CPP was defined as the equation CPP = $v/a_0.l_c$, where v, l_c, and a_0 are, respectively, the volume and length of the lipophilic chain and the cross-section area of the hydrophilic core of the phospholipid expressed per molecule in the aggregates. And the amphiphilic molecules with a CPP value falling outside of the range will assemble into other shapes.

1.4 Phase Diagram:

A phase diagram can be used to illustrate the relationship between a mixture's composition and its phase behavior. Although the vast majority of systems are investigated under conditions of ambient pressure, compositional factors can also be evaluated as a function of temperature and pressure. A ternary phase diagram, in which every point of the figure represents 100% of a certain component, may be used to study the phase behavior of basic microemulsion systems composed of oil, water, and surfactant.

More commonly, however, and almost always in the case of microemulsions in pharmaceutical applications, the microemulsion will contain additional components such as a cosurfactant and/or drug. The cosurfactant is also amphiphilic with an affinity for both the oil and aqueous phases and partitions to an appreciable extent into the surfactant interfacial monolayer present at the oil–water interface. The cosurfactant need not necessarily be capable of forming association structures in its own right. A wide variety of molecules can function as cosurfactants including non- ionic surfactants, alcohols, alkanoic acids, alkanediols and alkyl amines.

In the case where four or more components are investigated, pseudo-ternary phase diagrams are used where a corner will typically represent a binary mixture of two components such as surfactant/ cosurfactant, water/drug or oil/drug. The number of different phases present for a particular mixture can be visually assessed.

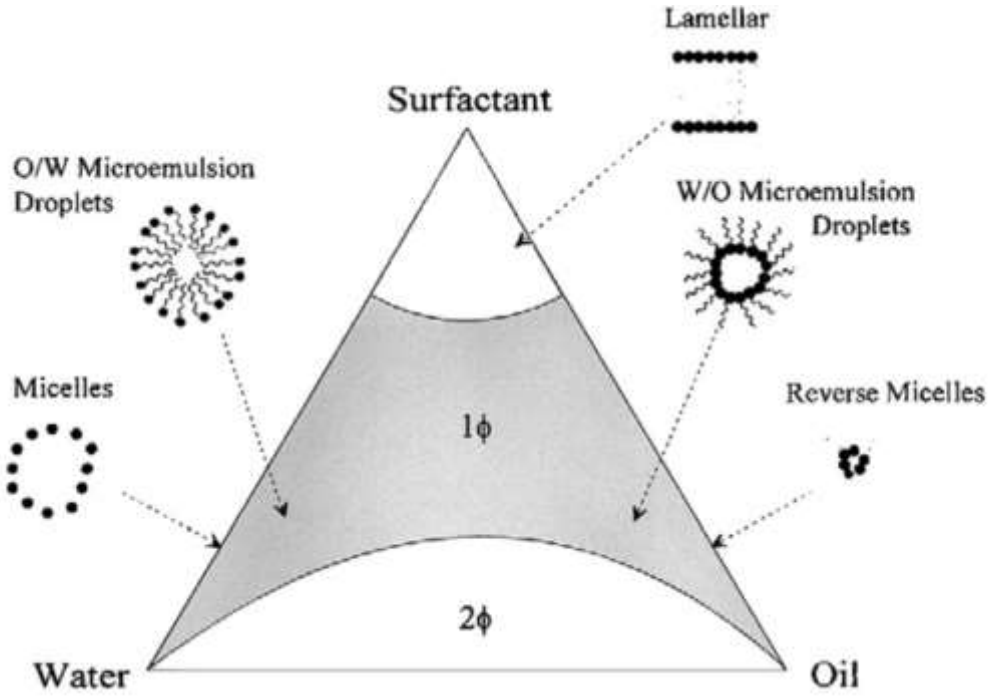

Fig1.4**:** pseudo-ternary phase diagram of an oil/ surfactant/water system with emphasis on microemulsion and emulsion phases **(**Lawrence, M. J.,et al.2012)

1.5 Statement of the problem and the objectives:

Pure curcumin is a chemically unstable hydrophobic substance with low water solubility—especially under acidic or neutral conditions where it remains fully protonated. It also shows poor chemical stability in alkaline environments and suffers from low bioavailability, primarily due to its poor bioaccessibility and rapid transformation by metabolic enzymes in the digestive tract. Moreover, curcumin is prone to degradation during storage when exposed to light, elevated temperatures, or alkaline pH. Although curcumin is relatively resistant to chemical degradation under acidic conditions, such environments often promote its crystallization and sedimentation in aqueous delivery systems due to its extremely low solubility in water.

To address these challenges, this study focused on formulating a curcumin-loaded microemulsion system to enhance its solubility and stability. A pseudo-ternary phase diagram was constructed to identify the microemulsion region in which curcumin is solubilized with the aid of a surfactant and co-surfactant. In addition, sixteen microemulsion samples were prepared in test tubes with varying curcumin concentrations to evaluate the influence of temperature on curcumin solubility in a water–oil mixture. Based on these experimental results, a fish-cut diagram was developed to identify the compositional and thermal regions in which curcumin remains solubilized. This systematic approach provides valuable insight into optimizing curcumin delivery systems for pharmaceutical and cosmetic applications.

Chapter Two:

Literature Survey:

Canales,L .et al(2023) in his study Curcumin was formulated in microemulsions based on oleic acid (oil phase), Tween® 80 (surfactant), and Transcutol® HP (cosurfactant). The microemulsion formation area was mapped by constructing pseudo-ternary diagrams for surfactant: co-surfactant ratios 1:1, 1:2, and 2:1. Microemulsions were characterized through measurements of specific weight, refractive index, conductivity, viscosity, droplet size, and in vitro skin permeation studies, as a result Nine microemulsions were prepared and characterized, showing clear, stable formulations with globule size dependent on the proportion of the components. The microemulsion with the highest loading capacity (60 mg/mL), based on Tween® 80, Transcutol® HP, oleic acid, and water (40:40:10:10) was able to penetrate the viable epidermis, finding a total amount of curcumin in the receptor medium at 24 h of 10.17 ± 9.7 μg/cm^2. The distribution of curcumin in the skin, visualized by confocal laser scanning microscopy, showed that the maximum amount was located between 20 and 30 μm.

Dourado, D. et al. (2022) This study aimed to develop a low surfactant concentration curcumin-loaded microemulsion (Curc-ME) having a gastrointestinal pH resistance, intended to prospect its oral use for further curcumin release. The effect of excipients on the apparent solubility of curcumin was assessed and a pseudo ternary phase diagram was designed to produce a low-surfactant microemulsion (ME) system. Curcumin was incorporated into the ME (Curc-ME), and the system was further physicochemically and physically characterized. The entrapment efficiency (EE) was determined by UHPLC. The systems' stability under storage, and its stability and curcumin release in simulated gastrointestinal fluids (SGIF) were evaluated. The excipients of the ME improved curcumin's apparent solubility. Curc-ME, stabilized with 15% of surfactants, displayed spherical droplets (sized of 21.81 ± 0.20 nm), polydispersity index of 0.07 ± 0.01, viscosity of 5.33 × 10−3 ± 0.01 Pa.s, conductivity of 160 ± 3 μS cm−1, surface tension of 40.37 ± 0.48 dynes/cm and EE of 98 ± 0.73%. Thermal analyses confirmed curcumin entrapment in the core of the system. The system remained stable over 90 days under storage and

under SGIF conditions. Curc-ME revealed a modified and complex kinetics release of curcumin in the SGIF. Overall, the results demonstrate that Curc-ME increased the solubility of curcumin, was produced with a remarkable low surfactant concentration, and showed stability and modified curcumin release at the gastrointestinal tract pHs. Therefore, Curc-ME revealed to be a promising candidate to be further explored as a therapeutic agent.

Amuti,et. al (2021),focuced in increase the water solubility and antioxidative stability of the curcumin, oil-in-water (O/W) and water-in-oil-in-water (W/O/W) microemulsions (MEs) were created. Particle size, polydispersity index (PDI), transmission electron microscopy, viscosity, and electrical conductivity measurements were used to describe MEs. Additionally, the antioxidant activity of MEs and curcumin's in vitro release were examined, and the location of curcumin in MEs was analyzed using proton nuclear magnetic resonance spectroscopy (1H NMR). 1H NMR indicated that curcumin is incorporated in the inner structure of MEs, and curcumin-loaded MEs were composed of spherical droplets with a mean particle size of 10.0–20.0 nm and a PDI of 0.2–0.3. Overall, it was shown that the MEs synthesized for this research significantly increased curcumin's solubility. Furthermore, evaluation of the two experimentally synthesized MEs' in vitro release and storage stability revealed that W/O/W ME exhibited higher sustained release and antioxidant activity than O/W ME. For the two ME that were examined, there were no discernible changes between storage at 4 °C and 25 °C. their research demonstrated that O/W and W/O/W MEs were excellent candidates to deliver curcumin.

Scomoroscenco, C. et al. (2021) This study aimed to develop and characterize new gel microemulsions suitable for topical cosmetic applications, using grape seed oil as the oily phase. Tween 80 and Plurol® Diisostearique CG were mixed to create the optimum microemulsion, and ethanol was used as a co-solvent. To improve the viscosity of the microemulsion, three different water-soluble polymers—Carbopol® 980 NF, chitosan, and sodium hyaluronate salt—were used. Every substance utilized is secure, biocompatible, and degradable. The medicine used as a model was turmeric. By using electrical conductivity, dynamic light scattering, polarized microscopy, and rheometric studies, the resulting systems were physically and chemically investigated. By using the MTT test, the cytotoxicity was evaluated. In the final phase of the study, the release behavior of Curcumin from the optimized microemulsion and two gel microemulsions was evaluated. The obtained gel microemulsions could be effective systems for incorporation and controlled release of the hydrophobic active ingredients.

Lin, C. C.et al (2009) Lecithin and Tween 80 served as the surfactants in the curcumin-encapsulated O/W microemulsion system, while ethyl oleate served as the oil phase. The ternary phase diagram of the system was created. Curcumin in microemulsion's stability and characteristics were looked at. UV-Vis spectra and diameter distributions showed that a curcumin microemulsion composition (DI water: surfactants (the mole ratio of lecithin/Tween 80 was 0.3): EO = 10: 1.7: 0.4 in wt. ratio) was stable for two months with an average diameter of 71.8 2.45 nm. For 48 hours, the microemulsion can be diluted with aqueous buffer without losing its structure This contribution also includes a skin permeation investigation for evaluating the penetration impact of different curcumin loads in microemulsions with varying particle sizes.

Vollmer, D.et al (1999) This study has developed a straightforward method for calculating phase diagrams based on temperature and composition. This approach provides a

semiquantitative prediction of key regions within the phase prism, including the phase boundaries of the three-phase (3ϕ) region, and is applicable to both weak and strong surfactants.
The model incorporates several essential parameters: the temperature-dependent changes in preferred curvature toward oil ($\mathbf{a_o}$) and water ($\mathbf{a_w}$), the volume fraction of the hydrophilic head group of the surfactant molecule ($\mathbf{x\Phi_s}$), the radii of oil micelles ($\mathbf{R^{oil}}_{mic}$) and inverse (water) micelles ($\mathbf{R^{w}}_{mic}$), and the temperatures that define the maximum extent of the three-phase region ($\mathbf{T_l}$ and $\mathbf{T_u}$).

Alkhaldi .M .et al.(2025) Different CUR ME formulations were developed, showing that decreasing oil and increasing water and surfactant content led to smaller particle size, lower PdI, and reduced zeta potential. Microemulsions significantly improved curcumin skin penetration compared to non-microemulsion formulations. The composition played a key role, with formulations containing higher surfactant and lower oil content achieving the highest penetration.

In comparison with the reviewed literature, my thesis shares several similarities with previous works, particularly in the general objective of enhancing the solubility and delivery of curcumin through microemulsion systems. Similar to earlier studies, the present work employed oil (oleic acid), nonionic surfactants (Span 80 and Tween 20), and ethanol as a co-surfactant, and utilized pseudo-ternary phase diagrams to identify one-phase regions capable of solubilizing curcumin. All studies, including this one, confirmed that microemulsions significantly improve the solubility of curcumin and hold promise for pharmaceutical and cosmetic applications. However, the present study differs from most previous works by integrating both theoretical and experimental approaches. Unlike earlier studies that focused mainly on physicochemical characterization and skin or oral delivery performance, this research applied Vollmer's model (1999) and developed a fish-cut diagram to analyze the relationship between temperature, composition, and solubility. Furthermore, theoretical calculations such as droplet radii (R_w and R_o), surfactant monolayer thickness, and emulsification boundaries (T^{web} and T^{oeb}) were carried out to complement experimental findings. These analyses revealed monotonic trends in droplet size with increasing water or oil fraction, and a linear increase of T^{web} with Φ_A accompanied by a decreasing trend of T^{oeb}, providing deeper insights into microemulsion behavior. Thus, while aligned with previous findings in demonstrating improved solubility and stability, this work is distinguished by its unique combination of experimental validation and theoretical modeling, offering a more comprehensive understanding of curcumin-loaded microemulsions.

Chapter Three:

Methods

3.1 Experimental methods

3.1.1 Materials and Reagents:

- Curcumin extract (95.05%) from Palolea (a local Palestinian industrial company in Jericho)
- Ethanol 95%,
- Distilled water,
- Span® 80; CAS Number: 1338-39-2; EC Number: 215-663-3; Synonyms: Sorbitan,
- Tween 20 was purchased from Sigma Aldrich.
- Oleic acid

3.1.2 Instruments:

- Analytical balance SHIMADZU ATx324 320g in Balances (S-841)
- Water bath
- Vortex shaker
- Test tubes
- Dropper
- screw caps

3.1.3 Phase diagram:

- The pseudo ternary phase diagrams consisting of Oleic acid oil, water, surfactant, mixture was constructing using the water titration method.

- The phase behavior of the systems consisting of curcumin powder, water phase and Span 80 and Tween 20 (Surfactants1:1) was plotted on a phase tetrahedron whose apexes respectively represent the pure components.
- 3g of a mixture consisting of curcumin powder dissolved in 95% ethanol and Surfactant at different weight ratios - as it is shown in the table (1) - were prepared in glass test tubes with screw caps and stirred at room temperature(25°C) by the vortex.

Table 3.1: **weight ratios of oil phase and A Mixture.**

Tube No.	A Mixture (g)	Oil phase(g)
1	0.1	0.9
2	0.2	0.8
3	0.3	0.7
4	0.4	0.6
5	0.5	0.5
6	0.6	0.4
7	0.7	0.3
8	0.8	0.2
9	0.9	0.1

The samples were titrated with the water phase as show in Table (2), While observing changes in the mixture's phases and recording the transition from a single phase to two or three phases (if such a transition occurs), Vortex shaker was used after each water addition, followed by a waiting period of approximately five minutes

3.1.4 Fish cut curve:

A binary combination of 8 g oleic acid and 2 g distilled water was created in 16 test tubes in order to examine the impact of temperature on phase behavior. Different amounts of a ternary surfactant-curcumin solution were introduced to each test tube.[(50 mL of Tween 20 and 50 mL of Span 80 were added after 3 g of curcumin was dissolved in 100 mL of 95% ethanol (A)] to create this solution.

The following amounts (in grams) of the curcumin-surfactant solution were added to the test tubes: 1.0, 2.0, 3.0, 4.0, 5.0, 6.0, 7.0, 8.0, 9.0, 10.0, 6.3, 6.5, 6.7, 7.2, 7.5, and 7.8 . To see the phase changes taking place in each sample, all 16 test tubes were exposed to various temperature settings. To investigate the effects of temperature and additive concentration on the mixture's phase behavior, observations were made, and fish cut was drawn using the model done by (Vollmer.D,1999).

3.2 Theoretical methods

3.2.1 The Preferred Curvature:

The temperature dependency of the preferred curvature of the surfactant monolayer toward water and oil must be taken into account in order to characterize the phase behavior. The radius of the droplets at the water and oil emulsification boundary is closely correlated with this curvature (Vollmer.D,1999).

The droplets reach their optimal size, or the opposite of the desired curvature, at the web and oeb. We first go over the mechanism that results in the development of the 2 ϕ -region upon crossing the emulsification barrier in order to highlight the connection between the desired curvature and droplet size. This research utilizes the fact that the mixture's microstructure is made up of droplets at the emulsification border, distant from the 3 ϕ -region.

The determinant of droplet size changes near the emulsification border, where temperature takes precedence over composition .

The behavior of the system is largely influenced by this distinctive dependency of the average droplet size on temperature and composition inside the 1 ϕ - and 2 ϕ -regions. Beyond the web, a water-rich phase and a microemulsion (ME) droplet phase coexist as the temperature rises. As the temperature rises, the volume of this water-rich phase grows until the majority of the water separates into this surplus phase.

3.2.2 Radius of droplets within the 1 and 2 ϕ-region

The radius R of monodisperse droplets in the 1,2 ϕ -region is entirely dependent on the volume fraction of the contained phase and surfactant. It depends only on the specified volume and surface area of the droplets and is not affected by temperature. Consistent with experimental results , volume and surface conservation suggest that the radii of oil and water droplets are determined by Eq(3.1a,3.1b). (Vollmer.D,1999).

$$R_w = \frac{3l_s[\Phi_w + x\Phi_A]}{\Phi_A} \qquad 3.1a$$

$$R_o = \text{`} - \frac{3\, l_s[\Phi_0 + (1-x)\Phi_A]}{\Phi_A} \qquad 3.1b$$

Where:

R_w :Radius of water droplet

R_o: Radius of oil droplet

l_s: Effective thickness of surfactant monolayer

Φ_A: Volume fraction of Surfactant+co.Surfactant+Curcumin.

Φ_w:Volume fraction of water

Φ_o: Volume fraction of oil

x: Surfactant head group volume ratio

The negative sign for the oil droplet radius for convenience in the phase boundary calculation that follows.

- **Effective thickness of surfactant monolayer(l_s) and head group volume ratio(x)calculation:**

  - 3 g of curcumin
  - 100 mL ethanol
  - 50 mL Span 80
  - 50 mL Tween 20

1. Convert volume to mass:

$$m = v * \rho \quad (3.2)$$

Where:

m:mass

v:volume

ρ:density

Using density for span80&Tween20 from , [Rowe et al., 2009]

For Span80:

50ml*1g/ml=**50g**

For tween20:

50ml*1.1g/ml=**55g**

2. Convert mass to moles

$$M = \frac{m}{M.W} \quad (3.3)$$

Where:

M :moles

m:mass

M. W:molecular weight

Molecular weight value from [Sigma-Aldrich, 2024]

For span80:

50/428.6=0.1167mol

For tween20:

55/1227.5=0.0448mol

3.Molar ratio and molar percentage:

$$\text{Total moles} = \text{Span80 moles} + \text{Tween20 moles} \quad (3.4)$$

0.1167+0.0448=0.1615 mol

Molar percentage:

$$\text{Molar\%} = (\text{Moles of component}/\text{Total moles}) * 100 \quad 3.5$$

For span80:

(0.1167/0.1615)*100=**72.3%**

For tween20:

(0.0448/0.1615)*100=**27.7%**

1. **Weighted Averages:**

4.1Effective thickness (l_s):

$$l_{s=}(\text{Span80\%} * l_s^{San80}) + (\text{Tween20\%} * l_s^{Tween20}) \quad 3.6$$

ls=0.723×26+0.277×23

=18.798+6.371=**25.17A**$^{\circ}$

Effective thickness value for Span80&Tween20 from [Kawakami, 2002]

4.2 Head Group Volume:

$$V_{head=}(\text{Span80\%} * V_{head}^{Span80}) + (\text{Tween20\%} * V_{head}^{Tween20}) \quad 3.7$$

V_{head}=0.723×150+0.277×450
=108.45+124.65=**233.1A**$^{\circ 3}$
Head Group Volume value as in[Kunieda & Shinoda, 1985]

Total Molecular Volume:

$$V_{Total} = (\text{Span80\%} * V_{total}^{Span80}) + (\text{Tween20\%} * V_{total}^{Tween20}) \quad 3.8$$

Vtotal=0.723×530+0.277×1250
=383.19+346.25=**729.4A**$^{\circ 3}$

2. **Head Group Volume Ratio(x):**

$$\text{Head group ratio} = V_{head}/V_{Toatal} \quad 3.9$$

233.1/729.4=0.3195≈ **0.32**

- **Volume fraction of (A, water and oil) (Φ_A, Φ_w, Φ_o) calculations:**

- $v = \frac{m}{\rho}$ 3.10

- $Tv = V_A + Vw + Vo$ 3.11

- $\Phi_A = \frac{VA}{Tv}$ 3.12
- $\Phi_{w=\frac{Vw}{Tv}}$ 3.13
- $\Phi_{o=\frac{Vo}{Tv}}$ 3.14

Where:

v:volume

m:mass

ρ:density

Tv:Total volume

V_A:volume of Surfactant+co.Surfactant+Curcumin.

Vw:Volume of water

Vo:Volume of oil

- Mass of oil=2g
- Mass of water=8 g
- A mass ranged from 1 to 10 grams
- Density of (A,W,O)=(**9**,**0.895**,**0.998**) respectively.

Calculating emulsification boundaries

$$T^{web} = T_l - \frac{1}{a_w}\ln\left(1 - \frac{R^w_{mic}}{3l_s}\frac{\Phi_A}{\Phi_w + x\Phi_A}\right) \quad 3.15a$$

$$T^{oeb} = T_u + \frac{1}{a_o}\ln\left(1 - \frac{\left|R^{oil}_{mic}\right|}{3l_s}\frac{\Phi_A}{\Phi_o + (1-x)\Phi_A}\right) \quad 3.15b$$

Where:

T^{web}: Temperature related to water emulsification boundary
T^{oeb}: Temperature related to oil emulsification boundary
T_1: Low temperature, the lowest temperature at which a microemulsion expels water.
T_u: Up temperature , the highest temperature where the 3ϕ region appears.
a_w: The change of the optimal radius of water with temperature

a_o: The change of the optimal radius of oil with temperature

R^w_{mic} : The radii of water micelles

R^{oil}_{mic}: The radii of oil micelles

Despite its continuous water-oil structure, Eq. (3.15) unexpectedly correctly defines the phase boundaries of the 3ϕ-region. It does this by describing the droplet size dependency on temperature in the 1ϕ and 2ϕ areas. the monolayer locally resembles droplet pieces of ideal size close to these boundaries. Furthermore, Eq. (3.15) demonstrates that seven material constants determine all emulsification boundaries in the Gibbs phase prism: the upper and the lower bound of the 3 ϕ-region T_l, T_u, respectively،the dimensionless micellar radii $R^{w}_{mic}\, l_s^{-1}$ and $R^{\text{oil}}\, l^{-\text{mic}}{}_{s}$ ،the change of the optimal radius with temperature a_w and a_o, and the volume fraction of the hydrophilic head group of a surfactant molecule x.

a_w and a_o were chosen based on values found in the literature to characterize the temperature sensitivity of micellar size in water-rich and oil-rich phases, respectively. The ranges of a_w and a_o for Tween 80 and oleic acid are 0.018 and 0.025 K^{-1} and 0.010 and 0.015 K^{-1}, respectively.

Chapter Four:

Result and discussion:

4.1 Introduction:

This section presents and analyzes the findings related to the formulation of curcumin-loaded microemulsions. A pseudo-ternary phase diagram was developed to identify the one-phase microemulsion region. Water titration was performed to map the phase behavior across varying compositions of oleic acid (oil) and surfactants (Tween 20 and Span 80). Phase boundaries were determined based on visual indicators of clarity and homogeneity, and specific compositions were selected to delineate the solubility limits.

In addition, the temperature-dependent behavior of the system was investigated using the fish-cut method. This included analysis of the water emulsification boundary (T_{web}), oil emulsification boundary (T_{oeb}). The influence of surfactant concentration on the size of micelles was also examined to evaluate its effect on system stability and emulsification behavior.

4.1 Pseudo Ternary Phase diagram :

Table 4.1: Phase Behavior Observed During Water Titration of Oil–Surfactant Mixtures at Varying Compositions.

Tube No.	Water mass (g)	Water (%)	Oil (%)	Surfactant (%)	Phase formed
4	0.9000	47.37	21.05	31.57	One phase
4	0.9973	49.93	20.02	30.04	Two phase
5	0.6000	37.50	31.25	29.66	One phase
5	0.6859	40.68	29.66	29.66	Two phase
7	0.4000	28.57	50.00	21.42	Two phase
7	0.4883	32.81	47.03	20.16	Three Phase
8	0.4000	28.57	57.14	14.29	Two phase
8	0.4330	30.22	55.83	13.96	Two phase
9	0.4000	28.57	64.29	7.142	Two phase
9	0.4200	29.58	63.38	7.042	Three phase

The Solubility Region identified during the experiments are summarized in Table 3. These points were selected based on visual observations of phase clarity and homogeneity upon titration.

Table 4.2: Boundary Point Compositions Used to Construct the solubility region in the Ternary Phase Diagram:

Point	Water mass(g)	Water (%)	Oil (%)	Surfactant (%)
1	0	0	0	100
2	0	0	50	50
3	0.60	37.50	31.25	31.25
4	0.95	48.72	20.51	30.77
5	0.95	48.72	15.38	35.89
6	1	100	0	0
7	0	0	0	100

Based on these data, a ternary phase diagram was constructed and presented in Figure 4.1, using OriginPro software to illustrate the phase behavior of the system.

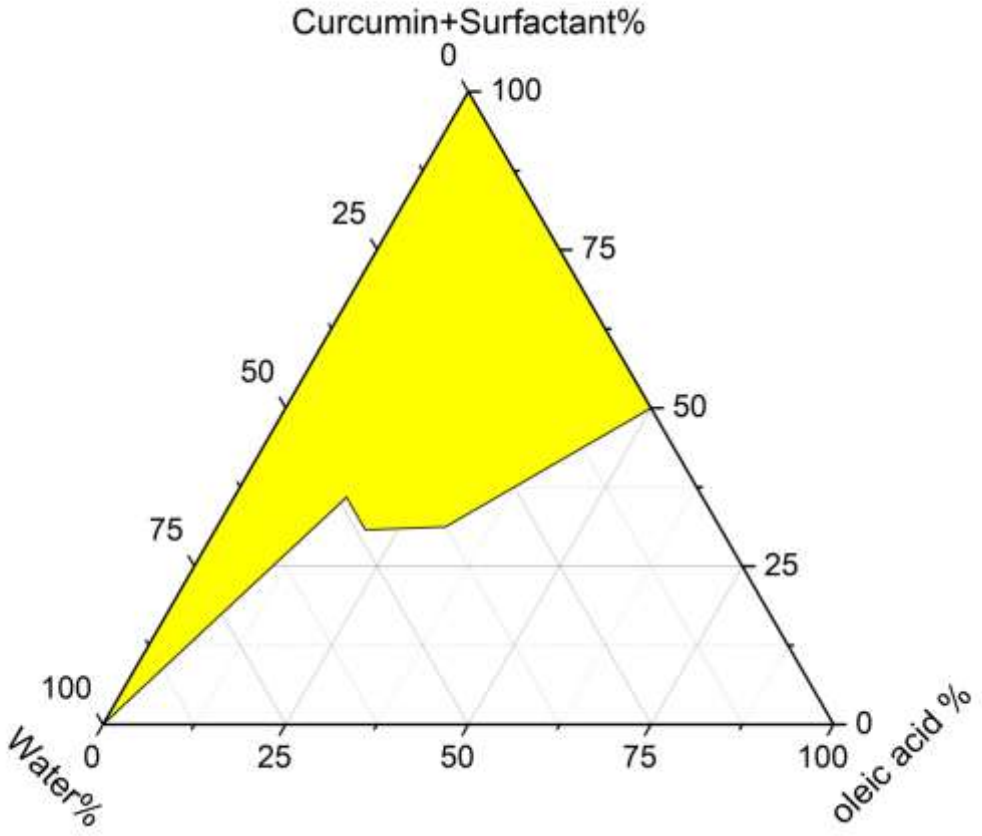

Fig 4.1: Pseudo Ternary Phase diagram of Curcumin, Water and oleic acid.

4.2 Fish cut curve for curcumin microemulsion

In Fish cut, three separate regions may be identified:
(1ϕ region): All water and oil can be dissolved by the microemulsion within the 1ϕ-region. Macroscopically, the combination is homogenous. Temperature, however, affects its microstructure.
(2ϕ region): Oil in water emulsion beneath the fish cut, and water in oil emulsion above the fish cut.
(3ϕ region): The surfactant is mostly dissolved in the middle phase (microemulsion), which coexists with phases that are mostly composed of water and oil, respectively, if the mixture separates into three phases.
The microemulsion phase expels water when the system crosses the top border out of the 1ϕ-region or the lower phase boundary into the 3ϕ -region, forming a water-rich phase alongside the existing phases. The temperature-dependent values of this phase barrier, known as the "water emulsification boundary" (web), are represented by T^{web}.
The microemulsion phase releases oil when it crosses the upper border into the 3ϕ area or the lower barrier out of the 1ϕ region, creating an oil-rich phase that coexists with the other phases. The temperature-dependent values of this barrier, known as the oil emulsification boundary (Oeb), are represented by the symbol (T^{oeb}).
In the Gibbs phase prism, the 3ϕ region extends between (T_l) and (T_u). (T_l) is the lowest temperature at which a microemulsion expels water, while (T_u) is the highest temperature where the 3ϕ region appears.
The values for T_l and T_u only depend on the choice of the water, oil, and surfactant.

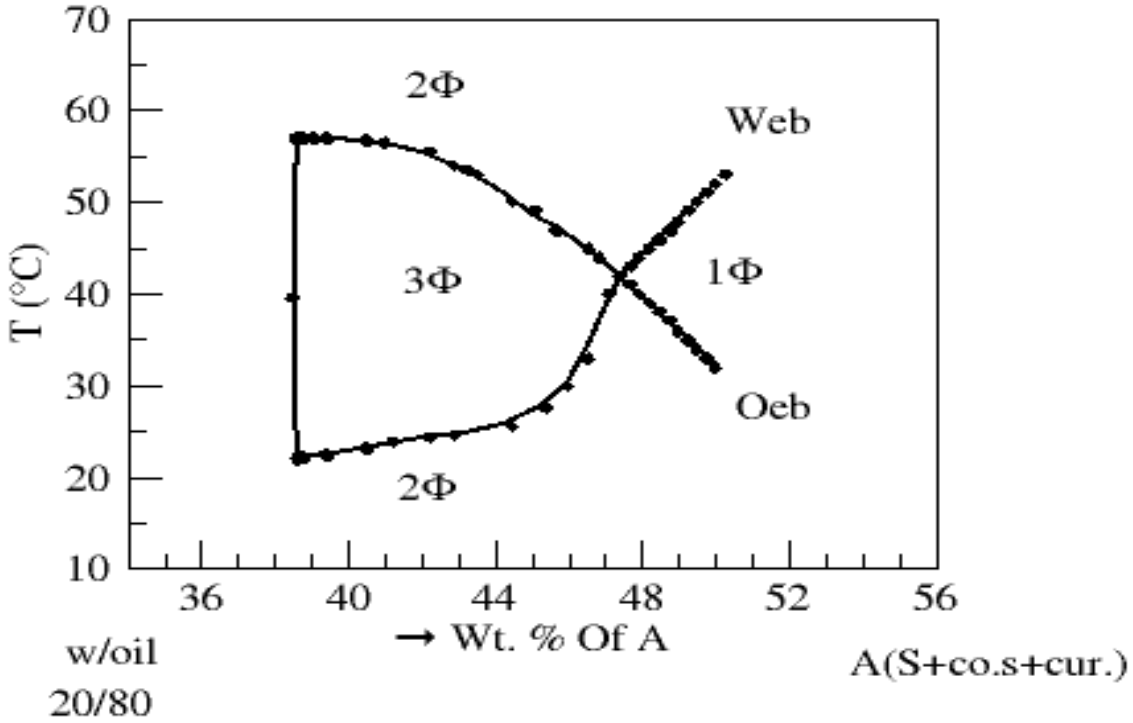

Fig. 4.2:Fish cut curve: sections through the phase prism for mixtures of H2O, oleic acid, and (Tween20+Span80+ethanol+curcumin). varying mass fraction of surfactant mix and fixed mass fraction of water and oleic acid (H2O/oil = 20:80)

4.3 Radius of Water and oil droplets within1 and 2 ϕ-region:

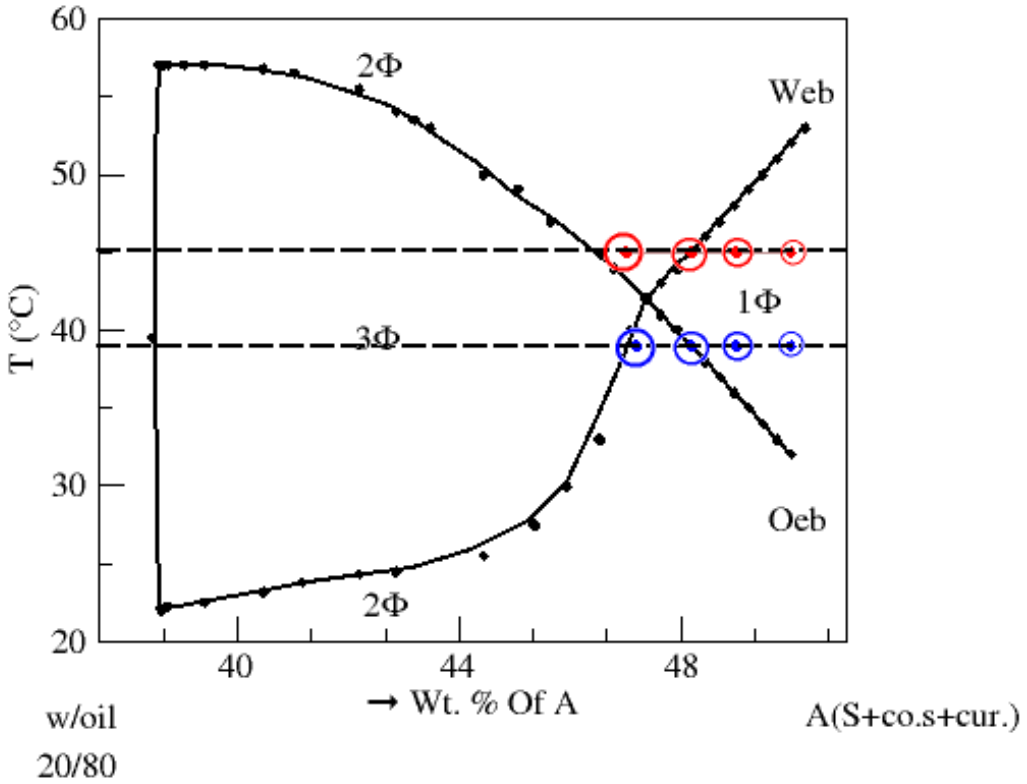

Fig. 4.3: different Wt. % of A at fixed temperature for oil (39 °C) and (45 °C) for water determined to calculate the radii of oil and water droplet in 1 and 2 ϕ-region.

From the fish-cut diagram, at a fixed temperature of 39°C for oil and 45°C for water, the radii of oil and water droplet (denoted as Rw and Ro) were calculated using Equations (3.1a) and (3.1b) at four different Wt. % of A. This calculation method follows the approach outlined by [Vollmer][1999], with X=0.32 and ls=25.2 Å.

Table 4.3: Variation of droplet radius for water (R_w) as a function of composition at 45°C.

Wt. % of A		Φ_w	Φ_A	R_W at **45 °C**
50	$\Phi_w < \Phi_w^{web}$	0.1693	0.075	17.37 ± 0.02
49	$\Phi_w < \Phi_w^{web}$	0.1696	0.074	17.69 ± 0.02
48.18	$\Phi_w = \Phi_w^{web}$	0.1698	0.073	17.97 ± 0.02
47	$\Phi_w > \Phi_w^{web}$	0.1701	0.071	18.35 ± 0.02

Table 4.4: Variation of droplet radius for water (R_o) as a function of composition at 39°C.

Wt. % of A		Φ_o	Φ_A	R_o at **39 °C**
50	$\Phi_o < \Phi_o^{oeb}$	0.755	0.075	-72.47 ± 0.03
49	$\Phi_o < \Phi_o^{oeb}$	0.756	0.073	-73.86 ± 0.03
48.18	$\Phi_o = \Phi_o^{oeb}$	0.757	0.072	-75.13 ± 0.03
47.2	$\Phi_o > \Phi_o^{oeb}$	0.758	0.071	-76.53 ± 0.03

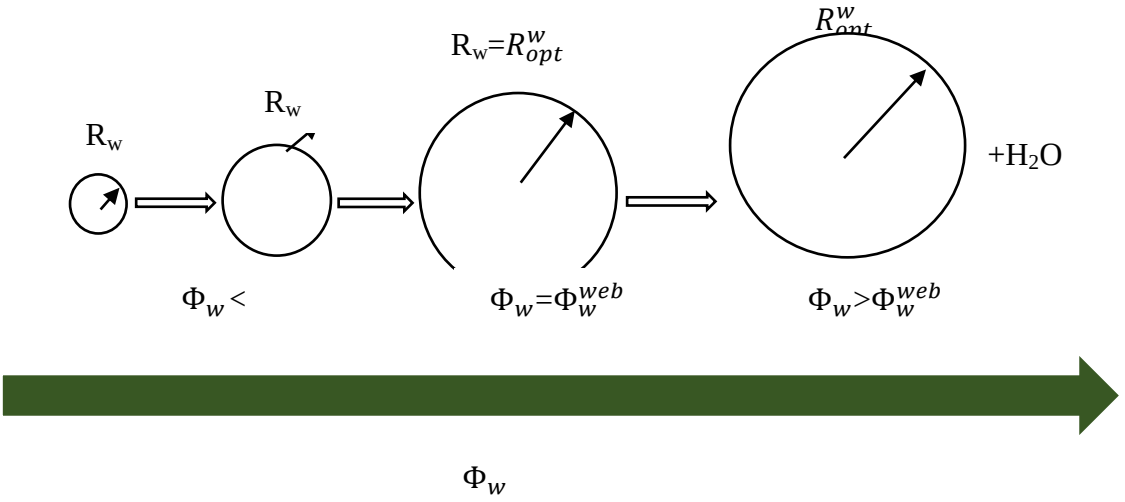

Fig 4.4: A graph of how a water droplet's size varies with its volume fraction at a fixed temperature.

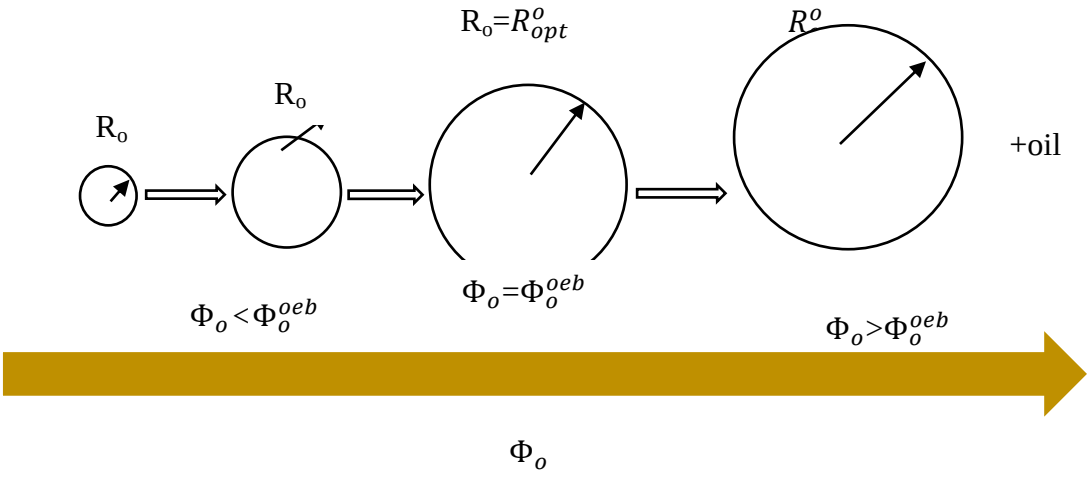

Fig. 4.5: A graph of how an oil droplet's size varies with its volume fraction at a fixed temperature.

The results illustrated in Figures 4.4 and 4.5 reveal a consistent, monotonic increase in both water (R_w) and oil (R_o) droplet radii as functions of volume fraction. Specifically, as the water volume fraction (Φ_w) increases at constant temperature, R_w begins at a low value and continues to increase steadily with increasing water content (Figure 4.4). Likewise, the oil droplet radius (R_o) shows a similar trend, increasing progressively as the oil volume fraction (Φ_o) rises (Figure 4.5). These observations indicate that droplet size expansion is continuously favored across the studied composition range, likely due to the gradual reduction in interfacial curvature and improved phase distribution.

This behavior is broadly consistent with the theoretical framework presented in Vollmer's study, *"How to calculate phase diagrams for microemulsions – a simple rule"* (1999), which explains how microemulsion domain sizes grow as systems approach favorable phase conditions. While Vollmer's model often anticipates non-monotonic trends around critical points, the current findings demonstrate that within the investigated range, both R_w and R_o increase without reversal, suggesting that the system does not reach or cross a critical curvature point.

The continuous growth in droplet radii supports the idea that structural evolution in microemulsions can follow a stable, increasing path as phase composition shifts. These results not only align with Vollmer's qualitative predictions but also offer quantitative evidence supporting droplet expansion under certain formulation conditions. Thus, the observed behavior reinforces and extends the theoretical understanding of microemulsion structuring in compositionally dynamic environments.

4.4 Emulsification boundaries

To determine $\frac{|R_{mic}^{oil}|}{l_s}$ **and** $\frac{R_{mic}^{w}}{l_s}$**,** equations (3.15a, 3.15b) were used**.**
T_l=22, T_u=57 (from fish cut), X=0.32

a_w and a_o were chosen according to research by Shinoda & Kunieda (1983) and Mitra & Dungan (2001), who examined microemulsion behavior in comparable surfactant and oil systems ; these values were obtained.

Table 4.5: The change of the optimal radius of (water/oil) with temperature (a_w, a_o) value

Parameter(K^{-1})	Phase	Surfactant/Oil	Typical Value(K^{-1})
a_w	Water-rich	Tween 80	0.018–0.025
a_o	Oil-rich	Oleic acid	0.010–0.015

From fish cut at different weights, of A take as in table 7 , Φ_A, Φ_w, Φ_o and calculated using equations (3.10,3.11,3.12,3.13,3.14), and T^{web} and T^{oeb} were determined for every single point.

Water weight and oil Weight are 2 g and 8g respectively.

Table 4.6: Normalized Radii of Water and Oil Micelles ($\frac{|R_{mic}^{oil}|}{l_s}$, $\frac{R_{mic}^{w}}{l_s}$)at Different Surfactant volume Fractions**.**

Wt. A(g)	Φ_A	Φ_w	Φ_o	T^{web} °C	T^{oeb} °C	$\frac{\|R_{mic}^{oil}\|}{l_s}$	$\frac{R_{mic}^{w}}{l_s}$
6.5	0.0658	0.730	0.2036	57	22	4.32 ± 0.02	16.70 ± 0.02
7	0.0705	0.727	0.2026	57	25	3.63 ± 0.02	14.91 ± 0.02
7.2	0.0724	0.725	0.2022	55	25	3.55 ± 0.02	13.89 ± 0.02
7.5	0.0751	0.723	0.2016	53	25	3.43 ± 0.02	12.75 ± 0.02
8	0.0798	0.719	0.2005	50	25	3.26 ± 0.02	11.09 ± 0.02

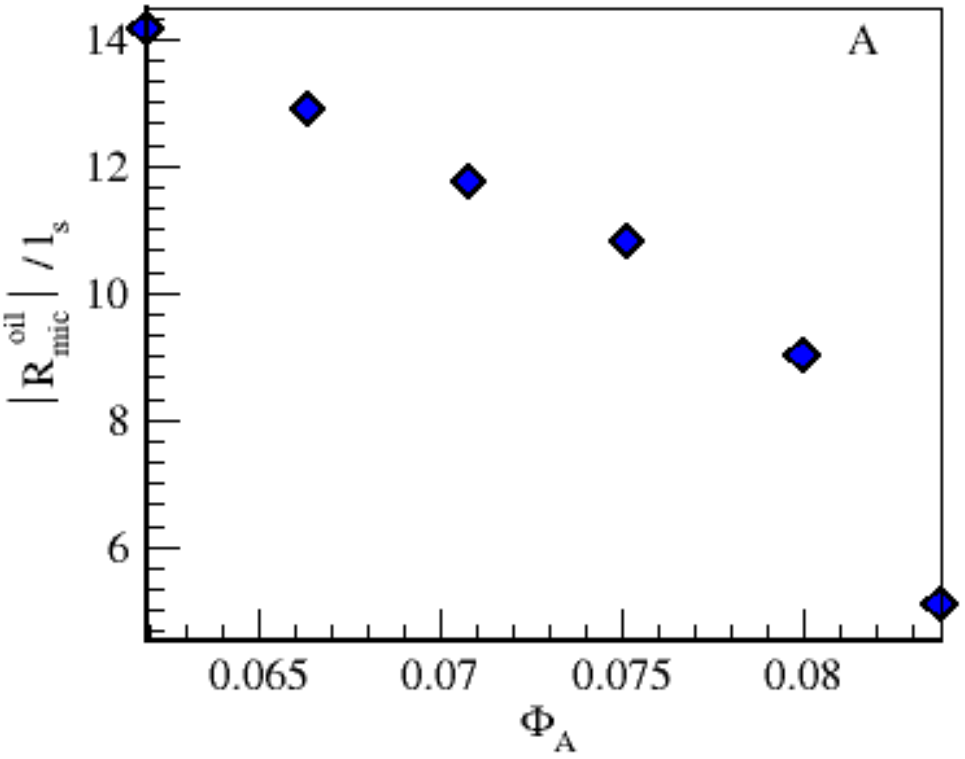

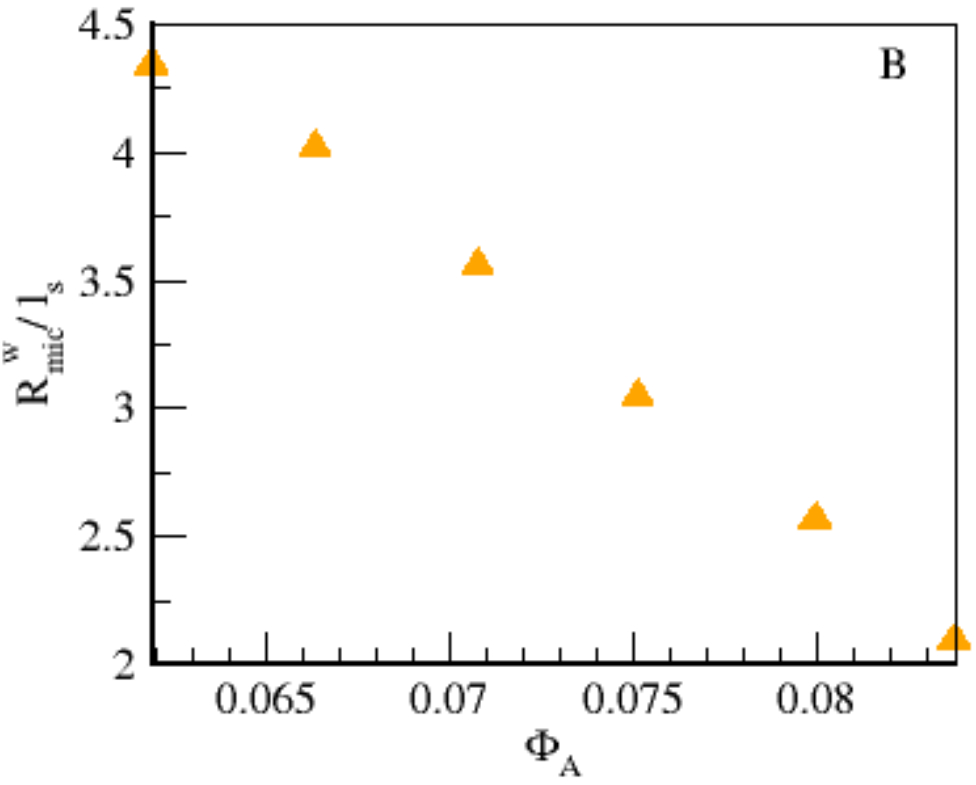

Fig. 4.6: (a) The radius of oil micelles R_{mic}^{oil}/l_s and (b) the radius of water micelles R_{mic}^{w}/l_s as a function of A volume fraction Φ_A

The observed trends in Figures 4.6.a and 4.6.b, showing a decrease in both oil and water micelle radii R_{mic}/l_s with increasing A volume fraction Φ_A, are consistent with the findings reported by Alkhaldi et al. (2025) in their experimental study on curcumin microemulsions. In that work, different formulations were evaluated to determine the influence of composition on droplet size and skin penetration. The authors demonstrated that increasing the surfactant content and decreasing oil content significantly reduced micelle size, resulting in improved dermal penetration efficacy.

This behavior parallels the current study's data, in which micellar size (both oil and water) showed a clear inverse relationship with Φ_A. The agreement between the two studies reinforces the conclusion that surfactant concentration is a key parameter controlling droplet radius and, consequently, formulation efficiency in curcumin-loaded microemulsion systems.

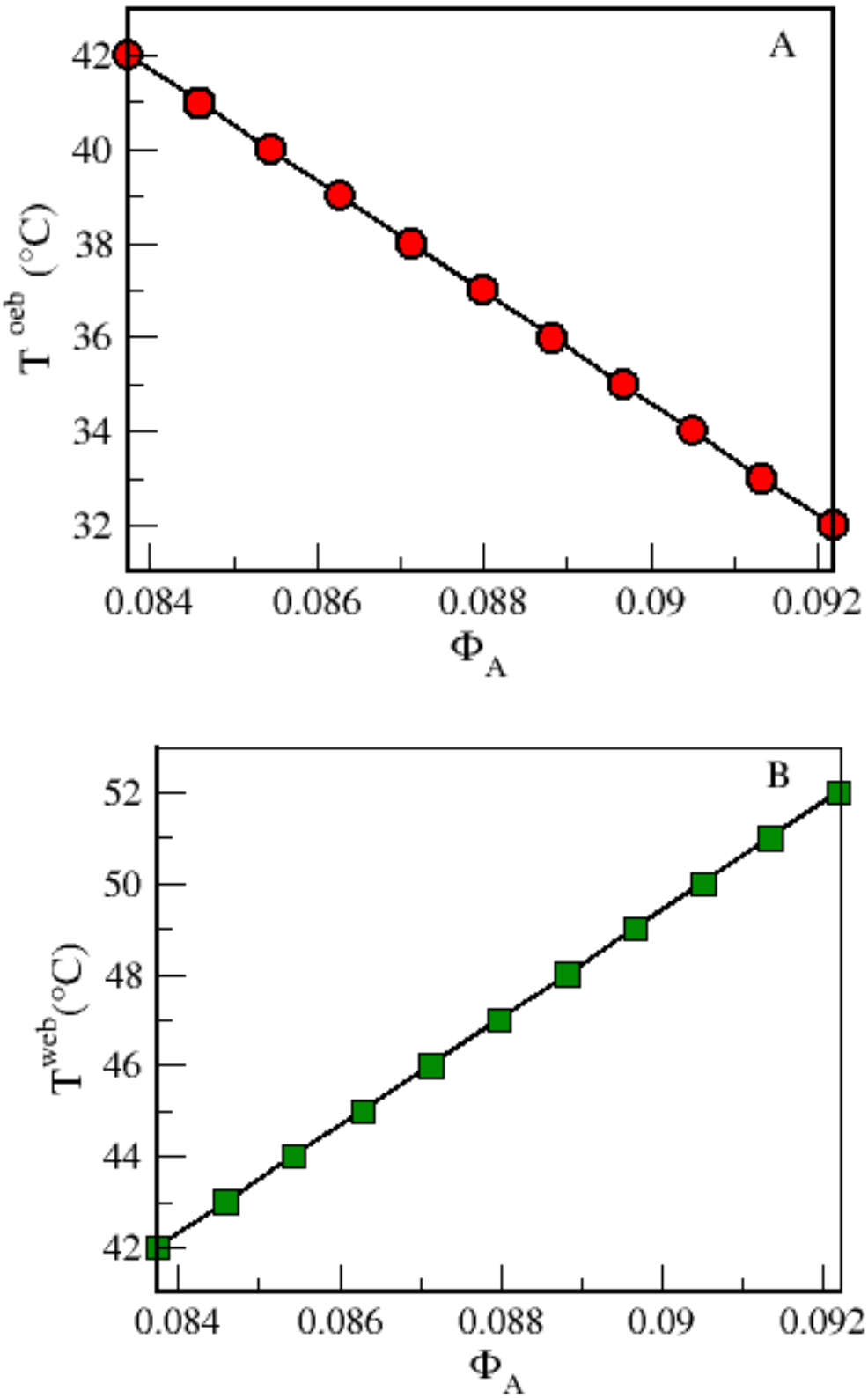

Fig. 4.7**:** The plot illustrates the relationship between (a) the oil emulsification boundary temperature T^{oeb} and the volume fraction of A, and (b) the water emulsification boundary T^{web} temperature and the volume fraction of A.

The trends observed in Figures 4.7.a and 4.7.b are in strong agreement with those reported by Vollmer (1999), who investigated the temperature boundaries of microemulsion systems using a similar fish-cut method. In his study, the water emulsification boundary T^{web} increased linearly with surfactant volume fraction, while the oil emulsification boundary T^{oeb} showed a decreasing trend, precisely as seen in the current system. This evidence supports the theoretical framework that surfactant concentration directly influences the curvature preference and thus the temperature at which phase separation occurs. The similarity in the behavior of T^{web} and T^{oeb} across different surfactant/oil systems validates the applicability of Vollmer's model to the curcumin-loaded microemulsion formulation in this study.

4.6 Discussion

- Alkhaldi and colleagues (2025) demonstrated that curcumin microemulsions significantly enhance dermal penetration compared to non-microemulsion controls in an ex vivo porcine ear model. Their systematic evaluation of nine formulations revealed that the composition is critical: lower oil content combined with higher surfactant and water content substantially improved curcumin's skin penetration efficacy. Specifically, the most effective formulation comprised 7.7 g of medium-chain triglycerides (MCT) as the oil phase, 6.92 g Tween® 80 plus 62.28 g ethanol as the surfactant mixture, and 23.1 g of water. Comparatively, the formulation with the highest water and Smix content (CUR ME 9) delivered curcumin with approximately 85% greater efficacy than the MCT oil formulation and about 50% higher penetration than the ethanol-only formulation.
  Moreover, physicochemical analysis showed that decreasing oil content while increasing surfactant and water levels corresponded with smaller droplet size, lower polydispersity index (PdI), and reduced zeta potential, all of which correlate with enhanced formulation stability and skin permeability.
  These findings highlight the pivotal role of microemulsion composition in optimizing the transdermal delivery of poorly water-soluble actives like curcumin and support the design of more effective topical delivery systems.
- In the curcumin microemulsion system, a distinct three-phase region was observed, with oil as the upper layer, water as the lower layer, and a middle microemulsion layer. This central microemulsion can be isolated by removing the excess phases and utilized directly in pharmaceutical applications, such as topical creams, transdermal gels, or oral delivery systems, enhancing curcumin's solubility, stability, and bioavailability.
- In the curcumin microemulsion system, non-ionic surfactants, specifically Tween 20 and Span 80, were employed to achieve high stability and effective curcumin delivery. Tween 20 (Polyoxyethylene sorbitan monolaurate) has a high HLB value (~16.7), making it strongly hydrophilic and suitable for stabilizing oil-in-water (O/W) microemulsions. In contrast, Span 80 (Sorbitan monooleate) has a low HLB (~4.3), favoring water-in-oil (W/O) systems due to its lipophilic nature. By combining these surfactants, a balanced HLB can be achieved, enabling the formation of stable curcumin-loaded microemulsions suitable for pharmaceutical applications.

  Non-ionic surfactants are widely recognized for their safety, being non-irritating, chemically stable, and compatible with various active compounds. They are commonly used in oral, topical, and transdermal formulations, ensuring safe and efficient delivery of bioactive compounds like curcumin.

4.7 Recommendations

Curcumin is a bioactive compound with significant therapeutic and health-promoting properties, including anti-inflammatory, antioxidant, and anticancer effects. In this study, a stable curcumin-loaded microemulsion was successfully developed with a curcumin concentration of 3%, demonstrating the potential of microemulsion systems to enhance curcumin solubility and bioavailability.

It is recommended that future work focus on optimizing microemulsion formulations to achieve higher curcumin loadings, up to 8%, while maintaining stability and desirable physicochemical properties. Increasing the curcumin content could further enhance its therapeutic efficacy and broaden its applications in pharmaceutical, nutraceutical, and functional food formulations.

Chapter Five:

Conclusion:

In this study, a curcumin-loaded microemulsion system was successfully developed using a nonionic surfactant blend (Span 80 and Tween 20), with ethanol as a co-surfactant and oleic acid as the oil phase, to address the major limitation of curcumin's poor water solubility. The system achieved effective solubilization of curcumin at a concentration of 3% (w/w), as demonstrated by the constructed pseudo-ternary phase diagrams, which identified several single-phase regions capable of incorporating curcumin into both aqueous and oil phases.

To further understand the phase behavior and solubilization characteristics, a fish-cut diagram was constructed following the approach of Vollmer (1999), revealing a distinct solubilization region, known as the "fish tail," across various curcumin concentrations and temperature conditions. Theoretical evaluation of droplet size in one-phase and two-phase regions showed that the water droplet radius (R_w) increased with water content at a fixed temperature of 45°C, while the oil droplet radius (Ro) was evaluated at 39°C. These findings reflect the structural response of the system to compositional variation.

Additionally, the upper and lower phase transition temperatures (T_u and T_l) and the Winsor boundary temperatures (T_{web} and T_{oeb}) were determined for both water and oil phases. Using calculated a_w and a_o values, the dimensionless micellar radii ($\frac{\left|R_{mic}^{oil}\right|}{l_s}$, $\frac{R_{mic}^{w}}{l_s}$) were analyzed within the three-phase region. A clear decreasing trend in micellar radius was observed with increasing volume fraction of component A (Φ_A). Furthermore, analysis of the fish tail region revealed that T^{web} increased linearly with Φ_A, while T^{oeb} exhibited a decreasing trend, indicating a systematic and interpretable phase behavior.

Overall, the formulation demonstrated not only a significant improvement in curcumin solubility but also structural and thermodynamic behavior consistent with established microemulsion theories. The integration of theoretical modeling with experimental tools such as the fish-cut diagram proved to be an effective strategy for characterizing and optimizing microemulsion-based drug delivery systems.

References:

1. Akbar, M. U., Rehman, K., Zia, K. M., Qadir, M. I., Akash, M. S. H., & Ibrahim, M. (2018). Critical review on curcumin as a therapeutic agent: From traditional herbal medicine to an ideal therapeutic agent. *Critical Reviews in Eukaryotic Gene Expression, 28*(1), 17–24. https://doi.org/10.1615/CritRevEukaryotGeneExpr.v28.i110.1615/CritRevEukaryotGeneExpr.2018020088
2. Alkhaldi, M., Sengupta, S., & Keck, C. M. (2025). Curcumin microemulsions: Influence of compositions on the dermal penetration efficacy. *Pharmaceutics, 17*(3), 301.
3. Amuti, A., Wang, X., Zan, M., Lv, S., & Wang, Z. (2021). Formulation and characterization of curcumin-loaded microemulsions: Evaluation of antioxidant stability and in vitro release. *Journal of Molecular Liquids, 336,* 116881.
4. Bhosale, R. R., Osmani, R. A., Ghodake, P. P., Shaikh, S. M., & Chavan, S. R. (2014). Nanoemulsion: A review on novel profusion in advanced drug delivery. *Indian Journal of Pharmaceutical and Biological Research, 2*(1), 122.
5. Chanda, S., & Ramachandra, T. V. (2019). Phytochemical and pharmacological importance of turmeric (*Curcuma longa*): A review. *Research & Reviews: A Journal of Pharmacology, 9*(1), 16–23.
6. Dourado, D., de Oliveira, M. C., de Araujo, G. R. S., Amaral-Machado, L., Porto, D. L., Aragão, C. F. S., ... & do Egito, E. S. T. (2022). Low-surfactant microemulsion, a smart strategy intended for curcumin oral delivery. *Colloids and Surfaces A: Physicochemical and Engineering Aspects, 652,* 129720.
7. Dutt, S., Siril, P. F., & Remita, S. (2017). Swollen liquid crystals (SLCs): A versatile template for the synthesis of nanostructured materials. *RSC Advances, 7*(10), 5733–5750.
8. Garti, N. (2008). *Delivery and controlled release of bioactives in foods and nutraceuticals.* Elsevier.
9. Ghosh, A., Banerjee, T., Bhandary, S., & Surolia, A. (2014). Formulation of nanotized curcumin and demonstration of its antimalarial efficacy. *International Journal of Nanomedicine, 9,* 5373.
10. Heger, M., van Golen, R. F., Broekgaarden, M., & Michel, M. C. (2014). The molecular basis for the pharmacokinetics and pharmacodynamics of curcumin and its metabolites in relation to cancer. *Pharmacological Reviews, 66*(1), 222–307.
11. Israelachvili, J. N. (2011). *Intermolecular and surface forces* (3rd ed.). Academic Press.
12. Israelachvili, J. N., & Mitchell, D. J. (1975). A model for the packing of lipids in bilayer membranes. *Biochimica et Biophysica Acta, 389*(1), 13–19.
13. Jin, T.-r. (2018). Curcumin and dietary polyphenol research: Beyond drug discovery. *Acta Pharmacologica Sinica, 39*(5), 779–786. https://doi.org/10.1038/aps.2017.179
14. Kawakami, K. (2002). Prediction of micelle formation of surfactants by molecular dynamics simulations. *Colloids and Surfaces B: Biointerfaces, 25*(3), 237–246.
15. Kharat, M., Du, Z., Zhang, G., & McClements, D. J. (2017). Physical and chemical stability of curcumin in aqueous solutions and emulsions: Impact of pH, temperature, and molecular environment. *Journal of Agricultural and Food Chemistry, 65*(8), 1525–1532.
16. Kunieda, H., & Shinoda, K. (1985). Evaluation of the head-group area of nonionic surfactants. *Journal of Colloid and Interface Science, 107*(2), 273–283.

17. Lawrence, M. J., & Rees, G. D. (2012). Microemulsion-based media as novel drug delivery systems. *Advanced Drug Delivery Reviews, 64,* 175–193.
18. Lee, J., Lee, Y., Kim, J., Yoon, M., & Choi, Y. W. (2005). Formulation of microemulsion systems for transdermal delivery of aceclofenac. *Archives of Pharmacal Research, 28,* 1097–1102.
19. Lin, C. C., Lin, H. Y., Chen, H. C., Yu, M. W., & Lee, M. H. (2009). Stability and characterization of phospholipid-based curcumin-encapsulated microemulsions. *Food Chemistry*, *116*(4), 923–928.
20. Lopresti, A. L. (2018). The problem of curcumin and its bioavailability: Could its gastrointestinal influence contribute to its overall health-enhancing effects? *Advances in Nutrition, 9*(1), 41–50. https://doi.org/10.1093/advances/nmx011
21. Luna-Canales, I. C., Delgado-Buenrostro, N. L., Chirino, Y. I., Nava-Arzaluz, G., Piñón-Segundo, E., Martínez-Cruz, G., & Ganem-Rondero, A. (2023). Curcumin-loaded microemulsion: Formulation, characterization, and in vitro skin penetration. *Drug Development and Industrial Pharmacy*, *49*(1), 42–51.
22. Maher, S. (2023). Safety of surfactant excipients in oral drug formulations. *International Journal of Pharmaceutics, 613,* 121–134.
23. McClements, D. J., Decker, E. A., & Weiss, J. (2007). Emulsion-based delivery systems for lipophilic bioactive components. *Journal of Food Science, 72*(8), R109–R124.
24. McClements, D. J., Decker, E. A., Park, Y., & Weiss, J. (2009). Structural design principles for delivery of bioactive components in nutraceuticals and functional foods. *Critical Reviews in Food Science and Nutrition, 49*(6), 577–606.
25. Mitra, S., & Dungan, S. R. (2001). Micellar and microemulsion properties of nonionic surfactants with vegetable oil. *Journal of Colloid and Interface Science, 235*(2), 386–394.
26. Nagarajan, R., & Ruckenstein, E. (1991). Theory of surfactant self-assembly. *Langmuir*, *7*(12), 2934–2969. https://doi.org/10.1021/la00060a020
27. Patel, R. M., & Patel, M. M. (2013). Formulation and evaluation of curcumin microemulsion for transdermal delivery. *Journal of Drug Delivery Science and Technology*, *23*(4), 351–359.
28. Priyadarsini, K. I. (2014). The chemistry of curcumin: From extraction to therapeutic agent. *Molecules*, *19*(12), 20091–20112.
29. Rahmani, A., Alsahli, M., Aly, S., Khan, M., & Aldebasi, Y. (2018). Role of curcumin in disease prevention and treatment. *Advances in Biomedical Research, 7,* 38. https://doi.org/10.4103/abr.abr_147_16
30. Rowe, R. C., Sheskey, P. J., & Owen, S. C. (2009). *Handbook of pharmaceutical excipients* (6th ed.). Pharmaceutical Press.
31. Saeidinia, A., Keihanian, F., Butler, A. E., Bagheri, R. K., Atkin, S. L., & Sahebkar, A. (2018). Curcumin in heart failure: A choice for complementary therapy. *Pharmacological Research, 131*, 112–119. https://doi.org/10.1016/j.phrs.2018.03.009
32. Schröder, C., Haberler, M., & Steinhauser, O. (2003). Journal of Molecular Liquids, 103–104, 85–105.
33. Scientific Spectator. (n.d.). The HLB system.
34. Sharma, R., Gescher, A., & Steward, W. (2005). Curcumin: The story so far. *European Journal of Cancer*, *41*(13), 1955–1968.
35. Shahidi, F., & Naczk, M. (2003). *Phenolics in food and nutraceuticals*. CRC Press.
36. Shinoda, K., & Kunieda, H. (1983). Phase transitions in systems of nonionic surfactants. *Journal of Colloid and Interface Science, 94*(2), 439–448.
37. Sigma-Aldrich. (2024). *Product data sheets for Span 80 and Tween 20.*

38. Smail, S. S., et al. (2021). Studies on surfactants, cosurfactants, and oils for microemulsion formulations. *Pharmaceuticals, 14*(5), 444.
39. Scomoroscenco, C., Teodorescu, M., Raducan, A., Stan, M., Voicu, S. N., Trica, B., ... & Cinteza, L. O. (2021). Novel gel microemulsion as topical drug delivery system for curcumin in dermatocosmetics. *Pharmaceutics, 13*(4), 505.
40. Tabrizi, R., Vakili, S., Akbari, M., Mirhosseini, N., Lankarani, K. B., Rahimi, M., ... & Asemi, Z. (2019). The effects of curcumin-containing supplements on biomarkers of inflammation and oxidative stress: A systematic review and meta-analysis of randomized controlled trials. *Phytotherapy Research, 33*(2), 253–262. https://doi.org/10.1002/ptr.6226
41. Teng, Y., Jin, H., Nan, N., Huang, J., & Zhang, H. (2020). Formulation of more efficacious curcumin delivery systems using colloid science: Enhanced solubility, stability, and bioavailability. *Foods, 9*(4), 430.
42. Tønnesen, H. H., Másson, M., & Loftsson, T. (2002). Studies of curcumin and curcuminoids. XXVII. Cyclodextrin complexation: Solubility, chemical and photochemical stability. *International Journal of Pharmaceutics, 244*(1-2), 127–135.
43. Ucisik, M. H., Küpcü, S., Schuster, B., & Sleytr, U. B. (2013). Characterization of curcuemulsomes: Nanoformulation for enhanced solubility and delivery of curcumin. *Journal of Nanobiotechnology, 11*, 1–13.
44. Van Os, N. M., Haak, J. R., & Rupert, L. A. M. (1993). *Physico-chemical properties of selected anionic, cationic and nonionic surfactants.* Elsevier.
45. Vollmer, D. (1999). How to calculate phase diagrams for microemulsions—A simple rule. *Lipid/Fett, 101*(10), 379–388.
46. Wang, N., Chen, M., & Wang, T. (2019). Liposomes used as a vaccine adjuvant-delivery system: From basics to clinical immunization. *Journal of Controlled Release, 303*, 130–150.
47. Zhang, Z., Zhang, R., Decker, E. A., & McClements, D. J. (2015). Development of food-grade filled hydrogels for oral delivery of lipophilic active ingredients: pH-triggered release. *Food Hydrocolloids, 44*, 345–352.
48. Zheng, B., & McClements, D. J. (2020). Formulation of more efficacious curcumin delivery systems using colloid science: Enhanced solubility, stability, and bioavailability. *Molecules, 25*(12), 2791.

تحضير ميكروواملشن للكركم

إعداد الطالبة: رغد زياد رشيد زغل

باشراف الدكتورة:د.خولة قمحية

المشرف الثاني:د.ابراهيم الكيالي

الملخص

في هذه الدراسة، تم تطوير نظام ميكرو مستحلب محمّل بالكركمين باستخدام مزيج من المواد الخافضة للتوتر السطحي غير الأيونية Span 80 وTween 20، مع الإيثانول كمساعد خافض للتوتر السطحي، وحمض الأوليبك كطور زيتي، وذلك بهدف التغلب على محدودية ذوبانية الكركمين في الماء. تم دمج الكركمين بتركيز 3 (w/w) %ضمن النظام، وتم إنشاء pseudo-ternary phase diagrams لتحديد مناطق الطور المفرد القادرة على إذابة الكركمين بكفاءة. وقد كشفت هذه المخططات عن عدة مناطق مميزة تؤكد فعالية النظام في تحسين ذوبانية الكركمين في الطورين المائي والزيتي.

ولفهم العلاقة بين التركيب ودرجة الحرارة وذوبانية الكركمين، تم بناء fish-cut diagramوفقًا لمنهجية Vollmer (1999). ومن خلال تحضير 16 عينة بمكونات مختلفة وخضوعها لدرجات حرارة متعددة، تم تحديد منطقة ذوبان واضحة تُعرف بمنطقة "ذيل السمكة"، مما يعكس استقرار التركيبة ضمن مدى واسع من التراكيب ودرجات الحرارة.

تم استخدام البيانات التجريبية لحساب أنصاف أقطار القطرات المائية (R_w) والزيتية (R_o) في منطقتي الطور الواحد والطورين. بالنسبة لـــRw ، تم التثبيت عند درجة حرارة 45 °C وأُخذت القياسات عند الكسر الحجمي المائي المقابل لنقطة تقاطع ذيل السمكة(Φ_w^{web}) ، بالإضافة إلى نقطتين سابقتين لها في منطقة الطورين ونقطة لاحقة في منطقة الطور الواحد. ولوحظ ازدياد في Rwمع زيادة محتوى الماء. وتم اتباع منهجية مماثلة لحساب Ro عند درجة حرارة 39.C°

كما تم تحديد درجات حرارة الانتقال الطوري العُليا (T_u) والدنيا(T_l) ، بالإضافة إلى درجات حرارة Winsor boundaryلكل من الماء والزيتT^{web} وT^{oeb} على التوالي. وبالاستناد إلى قيم a_wوa_o، تم حساب dimensionless micellar radiiلكل من الماء والزيت ضمن منطقة الأطوار الثلاثية، ممثلة بالصيغة $\frac{R_{mic}^{w}}{l_s}$, $\frac{|R_{mic}^{oil}|}{l_s}$ وقد أظهر تحليل العلاقة بين الكسر الحجمي للمكون A (Φ_A)و dimensionless micellar radiiاتجاهًا تنازليًا مع زيادةΦ_A ، مما يشير إلى تغير في البنية الميكروية للنظام.

علاوة على ذلك، أظهر تحليل منطقة "ذيل السمكة" أن T^{web} يزداد خطيًا مع ازدياد Φ_A ، بينما T^{oeb} يُظهر اتجاهًا تنازليًا. وقد دعم هذا السلوك المتناغم بين T^{web} و T^{oeb} عبر أنظمة مختلفة من المواد الخافضة للتوتر السطحي والزيوت موثوقية النتائج المُستخلصة.

بشكل عام، أظهرت النتائج أن الميكرو مستحلب المطور يُحسن بشكل كبير من ذوبانية الكركمين، مع سلوك بنيوي وثرموديناميكي يتماشى مع النظريات المعروفة في مجال الميكرو مستحلبات. كما أثبت الدمج بين النمذجة النظرية وتحليل fish-cut diagram فعاليته في تفسير خصائص النظام وتحسين تصميم أنظمة توصيل الدواء القائمة على الميكرو مستحلبات.

الكلمات المفتاحية: التحضير، ميكروامليشن، كركم.